The feeding system of *Tiktaalik roseae*: an intermediate between suction feeding and biting

Justin B. Lemberg[a] , Edward B. Daeschler[b], and Neil H. Shubin[a,1]

[a]Department of Organismal Biology and Anatomy, The University of Chicago, Chicago, IL 60637; and [b]Department of Vertebrate Zoology, Academy of Natural Sciences of Drexel University, Philadelphia, PA 19103

Changes to feeding structures are a fundamental component of the vertebrate transition from water to land. Classically, this event has been characterized as a shift from an aquatic, suction-based mode of prey capture involving cranial kinesis to a biting-based feeding system utilizing a rigid skull capable of capturing prey on land. Here we show that a key intermediate, *Tiktaalik roseae*, was capable of cranial kinesis despite significant restructuring of the skull to facilitate biting and snapping. Lateral sliding joints between the cheek and dermal skull roof, as well as independent mobility between the hyomandibula and palatoquadrate, enable the suspensorium of *T. roseae* to expand laterally in a manner similar to modern alligator gars and polypterids. This movement can expand the spiracular and opercular cavities during feeding and respiration, which would direct fluid through the feeding apparatus. Detailed analysis of the sutural morphology of *T. roseae* suggests that the ability to laterally expand the cheek and palate was maintained during the fish-to-tetrapod transition, implying that limited cranial kinesis was plesiomorphic to the earliest limbed vertebrates. Furthermore, recent kinematic studies of feeding in gars demonstrate that prey capture with lateral snapping can synergistically combine both biting and suction, rather than trading off one for the other. A "gar-like" stage in early tetrapod evolution might have been an important intermediate step in the evolution of terrestrial feeding systems by maintaining suction-generation capabilities while simultaneously elaborating a mechanism for biting-based prey capture.

cranial kinesis | feeding | tetrapodomorph | water-to-land transition

Although suction feeding is a primary mode of prey capture among aquatic vertebrates (1), it is physically impractical on land due to the lower viscosity of air as compared to water (2–4). Terrestrial-feeding vertebrates must resort to other means, such as biting or tongue capture, to procure food (2). Naturally, researchers seeking to understand shifts in feeding strategies in tetrapodomorph vertebrates during the water-to-land transition have focused primarily on whether feeding systems in fossil forms showed adaptations for either suction or biting (2, 5). Generally, plesiomorphic "fish-like" morphology is interpreted as a means to create suction during the feeding cycle, and derived "tetrapod-like" morphology is interpreted as suggestive of biting (5–8). Suction feeding in fish is typically associated with jointed, kinetic skulls that allow for large volumetric expansion to draw in food (1, 9). In contrast, many lineages of modern tetrapods have consolidated skulls, such as mammals, crocodilians, and amphibians, thought to strengthen the skull for biting (9–12). While there is evidence for kinetic joints in the palate and skull roof of multiple early stem tetrapods (6, 13–16), it is uncertain if they represent plesiomorphic holdovers of limited fish-like cranial kinesis (13, 17, 18) or were independently derived mechanisms to improve biting capabilities on land (17, 19).

A central challenge of paleontology has been to understand how, and when, transitions in the feeding system of early terrestrial vertebrates occurred. Late Devonian finned tetrapodomorphs, typified by *Eusthenopteron foordi*, have expansive, kinetic skulls with open sutures, robust gill covers, large hyomandibulae,

tall palatal elements, and a jointed neurocranium all thought to be features that play a role in suction feeding (5, 9, 20). In contrast, the Late Devonian limbed tetrapodomorph *Acanthostega gunnari* has a flat skull, interdigitating sutures between the bones of the skull roof, absent gill covers, reduced hyomandibulae, horizontal palatal elements, and a consolidated neurocranium that are hypothesized to be derived adaptations for biting (5, 6, 21, 22). Analyses of tetrapodomorph lower jaws have produced equivocal results, noting few differences between presumed aquatic and terrestrial forms (7, 8). These results suggest that either a fish-like suction-based feeding mechanism was maintained well into the Carboniferous (7, 8, 23) or that a biting-based feeding mechanism had evolved in water prior to the origin of terrestrial tetrapods (24).

To understand how feeding modes shifted among tetrapodomorphs and assess the origin of novel feeding mechanisms in the tetrapod lineage, we use high-resolution microcomputed tomography (μCT) to analyze multiple specimens of a well-preserved elpistostegalian-grade tetrapodomorph, *Tiktaalik roseae*, and compare the anatomy resolved from those μCT scans to features of other extinct tetrapodomorphs and extant fishes with analogous features. *T. roseae* is a tetrapodomorph from the Upper Devonian (Frasnian, ~375 Mya) of Arctic Canada (Ellesmere Island, Nunavut Territory) (25, 26) that, according to most-recent phylogenies (27, 28), is representative of the outgroup of limbed vertebrates (tetrapods). Although plesiomorphic in lower jaw morphology (7, 8, 29), elpistostegalian-grade

Significance

The water-to-land transition is a major event in vertebrate history, involving significant changes to feeding structures and mechanics. In water, fish often use suction-feeding to capture prey, but this feeding strategy is not possible on land. Therefore, it has been traditionally believed that the invasion of land involved a shift from suction-based prey capture to mechanisms based on biting and snapping. Computed tomography analysis of *Tiktaalik roseae*, a key intermediate in tetrapod evolution, compared with extant analogs (gars and polypterids), reveals a rigid skull, capable of biting, with joint morphologies suggestive of cranial kinesis and suction generation. An intermediate condition that utilizes both feeding strategies helps explain some of the key morphological changes in cranial anatomy during the water-to-land transition.

tetrapodomorphs (a group also including *Panderichthys rhombolepis* and *Elpistostege watsoni*) represent a period of rapid cranial evolution that could nevertheless suggest shifts in feeding strategies (5, 26, 30, 31). µCT was performed on four specimens of *T. roseae* from the Nunavut Fossil Vertebrate Collection (NUFV) consisting of three-dimensionally (3D) preserved palatal material in articulation with the cranium, as well as individual bones from multiple disarticulated specimens (*SI Appendix*, Table S1). Sutural cross-sections were compared with homologous sutures reported for *E. foordi* (5, 20) and *A. gunnari* (5, 21). Cranial joints were compared with possible modern analogs, alligator gar (*Atractosteus spatula*) (32–34) and ornate bichir (*Polypterus ornatipinnis*) (5, 32, 35), which were selected on the basis of convergent feeding morphologies with *T. roseae*. Finally, joints between the palate, hyomandibula, and braincase were modeled with the same kinematic range of motion as reported in *A. spatula* for comparison purposes (34).

Results

Sutural Morphology. Although sutures were visible in all the scans, sutures were best visualized from scans with lower voltage and higher resolution (*SI Appendix*, Table S1). Although not immediately apparent in all slices, sutures could be characterized along the midline and in the cheek of *T. roseae* (Fig. 1). Interdigitating sutures were most common in the dermal roofing bones of the skull table and along the midline of the rostrum. These sutures included the interpostparietal suture (Fig. 1A), the interfrontal suture (Fig. 1 B and C), and the parietal–postparietal suture (Fig. 1E). Interdigitations occur along the midline anterior and posterior to the pineal foramen, in a condition more

similar to *A. gunnari* than *E. foordi* (5). Often, boundaries of dermal bones immediately overlying the endochondral ossifications of the sphenethmoid and otoccipital were obscured (Fig. 1 A–C and F and *SI Appendix*, Fig. S1 A and B), suggesting heavy integration of skull roofing bones with the braincase. Sutures between bones of the external cheek were typically overlapping, beveled sutures, also similar to the condition reported in *A. gunnari* (21, 23). These sutures included the lacrimal–jugal (Fig. 1G), lacrimal–maxilla (*SI Appendix*, Fig. S1B), and jugal–postorbital (*SI Appendix*, Fig. S1C). Throughout the cranium, sutural joints were tightly bound together, lacked matrix in-fill, and were typically obscured from surface view due to dermal sculpting (Fig. 1).

In contrast to sutural joints, however, there is also a continuous series of overlapping joints running the length of the skull that separates the bones of the dermal skull roof and bones of the external cheek (Figs. 1 and 2B, magenta lines). These joints include the lacrimal–prefrontal (Fig. 1 D and H), postorbital–intertemporal (*SI Appendix*, Fig. S1C), and postorbital–supratemporal (Fig. 1F). These joints are typically separated, filled with lower-density matrix, and unobscured by dermal sculpting, which makes them prominently visible in dorsal surface views (Fig. 1). Anterior to the orbit, this division takes the form of a longitudinal scarf joint running rostrally to the external nares, parallel to the midline. This "rostral scarf joint" (Fig. 2B, "rsj") separates the lacrimal, jugal, and maxilla—bones typically associated with the external cheek (20)—from the prefrontal, premaxilla, and anterior tectal bones. Posterior to the orbit, this division continues in the form of a broad overlap of the postorbital with a shelf formed by the intertemporal and
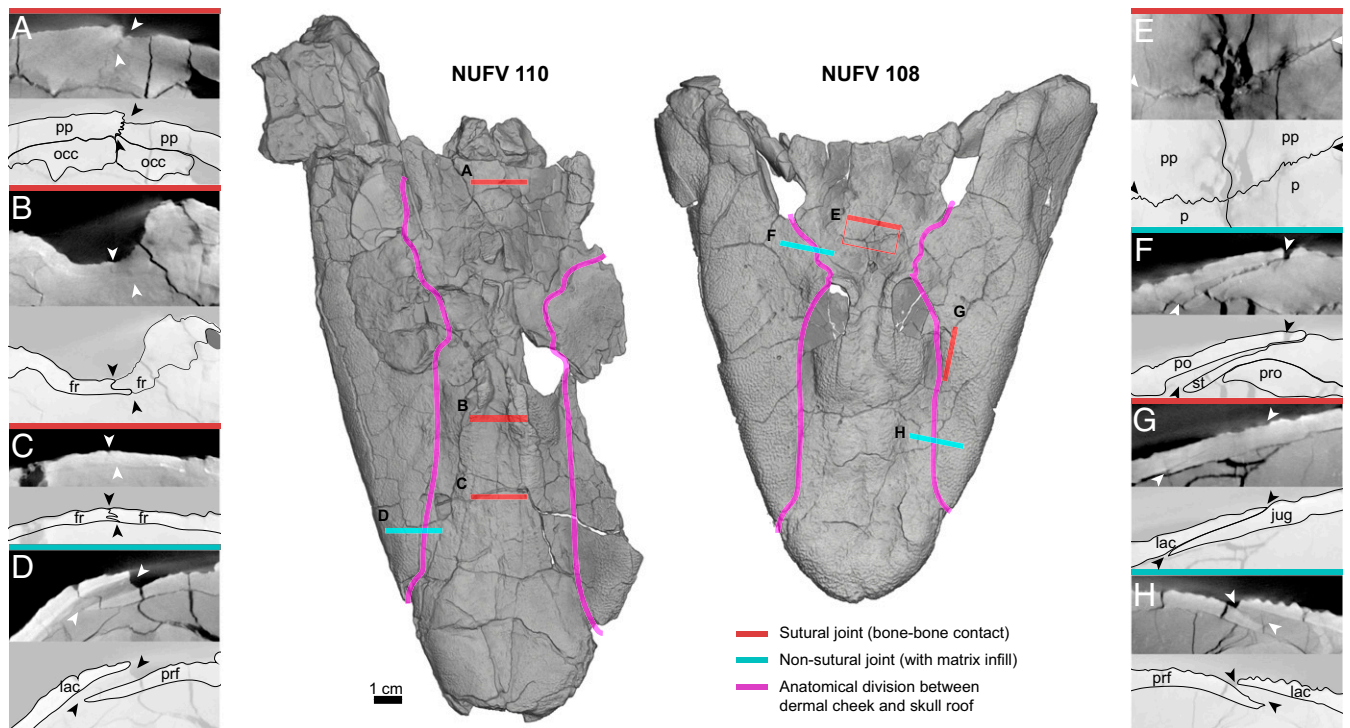

Fig. 1. Dermal joint patterns in the skull roof and cheek of *T. roseae*. Shown are dorsal views of skulls of NUFV 110 (*Left*) and NUFV 108 (*Right*) with 2-cm-width µCT cross-sections and line drawings of sutural (red, A–C, E, G) and nonsutural (cyan, D, F, and H) joints. Line drawings are used to omit details of µCT cross-sections such as scanning artifacts (localized brightening) and cracks (black lines, splotches). (A) Interpostparietal interdigitating suture; (B and C) interfrontal interdigitating suture; (D and H) nonsutural lacrimal–prefrontal scarf joint; (E) dorsal view of the interdigitating postparietal–parietal suture; (F) nonsutural overlapping postorbital–supratemporal joint that overlies the prootic buttress; and (G) sutural overlapping scarf joint at the lacrimal–jugal contact that contrasts with the loose overlap between the dermal cheek and braincase (magenta line). Arrowheads indicate beginnings and ends of sutures in µCT and line drawings. fr, frontal; jug, jugal; lac, lacrimal; occ, occipital; p, parietal; po, postorbital; pp, postparietal; prf, prefrontal; pro, prootic buttress; st, supratemporal.
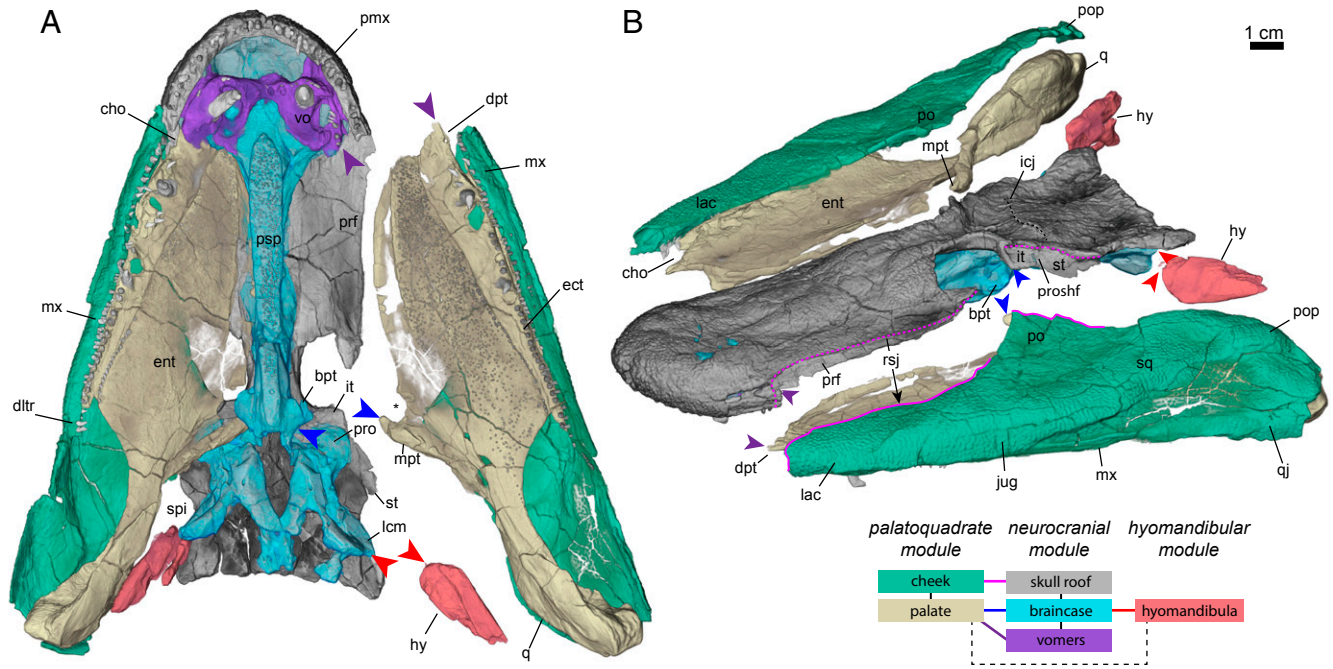
Fig. 2. Functional modularity of the skull of *T. roseae*. Disarticulated skull of *T. roseae* (NUFV 108) in ventral (*A*) and antero-dorsolateral (*B*) left oblique views. Bones of distinct regions are color-coded by anatomical unit: cheek (green), palate (yellow), skull roof (gray), braincase (cyan), vomers (purple), and hyomandibula (red). These anatomical units are further grouped into functional modules, which have clear mobile articulations with other modules but otherwise appear to be functionally integrated and immobile within themselves. Articulations of the palatoquadrate module (cheek and palate) with the neurocranial module (dermal skull roof, neurocranium, vomers) include the metapterygoid–suprapterygoid fossa (*SI Appendix*, Fig. S1C, blue arrow), dermopalatine–vomerine (*SI Appendix*, Fig. S1A, purple arrow), rostral scarf joint (*SI Appendix*, Fig. S1B, magenta line), and prootic shelf (Fig. 1F and *SI Appendix*, Fig. S1C, magenta line; see text). Articulation of the hyomandibular module (hyomandibula) with the neurocranial module is at the hyomandibula–lateral commissure (red arrow). Articulation of the palatoquadrate module with the hyomandibular module is presumably entirely cartilaginous. bpt, basipterygoid (asterisk marks corresponding medial notch of entopterygoid); cho, choana; dltr, distal-most teeth on the lateral toothrow; dpt, dermopalatine; ect, ectopterygoid; ent, entopterygoid; hy, hyomandibula; icj, intracranial joint; it, intertemporal; jug, jugal; lac, lacrimal; lcm, lateral commissure; mpt, metapterygoid; mx, maxilla; po, postorbital; pop, preopercle; prf, prefrontal; pro, prootic buttress; proshf, prootic shelf; psp, parasphenoid; q, quadrate; qj, quadratojugal; rsj, rostral scarf joint; spi, spiracle; sq, squamosal; st, supratemporal; vo, vomer.

supratemporal, which in turn are supported ventrally by the prootic processes of the braincase (Fig. 1F and *SI Appendix*, Fig. S1C, "pro"). This "prootic shelf" (Fig. 2B, "proshf") again separates bones of the external cheek from those of the skull roof.

Functional Modularity of the Skull. The crania of many groups of fishes are extensively jointed to enable separate movements between cranial elements, and the skull of *T. roseae* is no exception. In addition to the separation of dermal bones of the skull roof from the external cheek, the braincase also maintains unfused and presumably mobile articulations with the individual components of the suspensorium (palatoquadrate and hyomandibula; Figs. 2 and 3A). Lateral movements of the cheek and suspensorium are a key component of cranial expansion in modern fishes, but, typically, the suspensorium in actinopterygians is treated as a single functional unit (1, 36–38), whereas, in nondipnoan sarcopterygians with an intracranial hinge, it is treated as two (9, 39). The cranium of *T. roseae* appears to have three functional modules (named after their primary endochondral component but consisting of both endochondral and dermal bones): a single-fused "neurocranial module" and a subdivided suspensorium consisting of a "palatoquadrate module" and a "hyomandibular module" (Figs. 2 and 3A).

The neurocranial module of *T. roseae* is heavily consolidated, and consists of the dermal skull roof, braincase, parasphenoid, and vomers. Whereas sarcopterygians plesiomorphically possess a jointed braincase between the otoccipital and sphenethmoid

portions of the braincase (6, 20), these regions are fused together in tetrapods and limbed tetrapodomorphs (6). *T. roseae* shows the beginnings of this process, first by forming interdigitations at the parietal–postparietal suture [i.e., the intracranial joint sensu Jarvik (1980); Figs. 1E and 2B]. Second, the prootic processes (26), which support the intertemporal and supratemporal ventrally (Fig. 2A), span anteriorly to the parietal–postparietal suture line (Fig. 2B), indicating a lack of mobility between the anterior and posterior regions of the skull roof. Unlike later tetrapodomorphs (6, 19), the sphenethmoid is completely ossified along its length (*SI Appendix*, Fig. S1 A and B), and the vomers are firmly sutured to the underside of the still-ossified ethmoid portion (*SI Appendix, Fig. S1A*). The parasphenoid–sphenethmoid complex forms a rigid I-beam in cross-section (*SI Appendix*, Fig. S1B), similar to the condition reported in *A. gunnari* (23). Together, these features suggest the braincase, skull roof, and the midline roof of the mouth are all integrated together into a rigid inflexible unit.

The palatoquadrate module of *T. roseae* is similarly an integrated unit, composed of the bones of the palate (quadrate, metapterygoid, entopterygoid, ectopterygoid, dermopalatine) along with the closely associated bones of the external cheek (maxilla, lacrimal, jugal, quadratojugal, postorbital, squamosal, and preopercle). The palate forms two main articulations with the braincase. The anterior-most articulation of the palate with the braincase is formed by an anterior prong of the dermopalatine (Figs. 2A and 3A and *SI Appendix*, Fig. S1A, purple arrows), which sockets into the rear wall of the nasal capsule,

Lemberg et al.
The feeding system of *Tiktaalik roseae*: an intermediate between suction feeding and biting

PNAS | 3 of 10
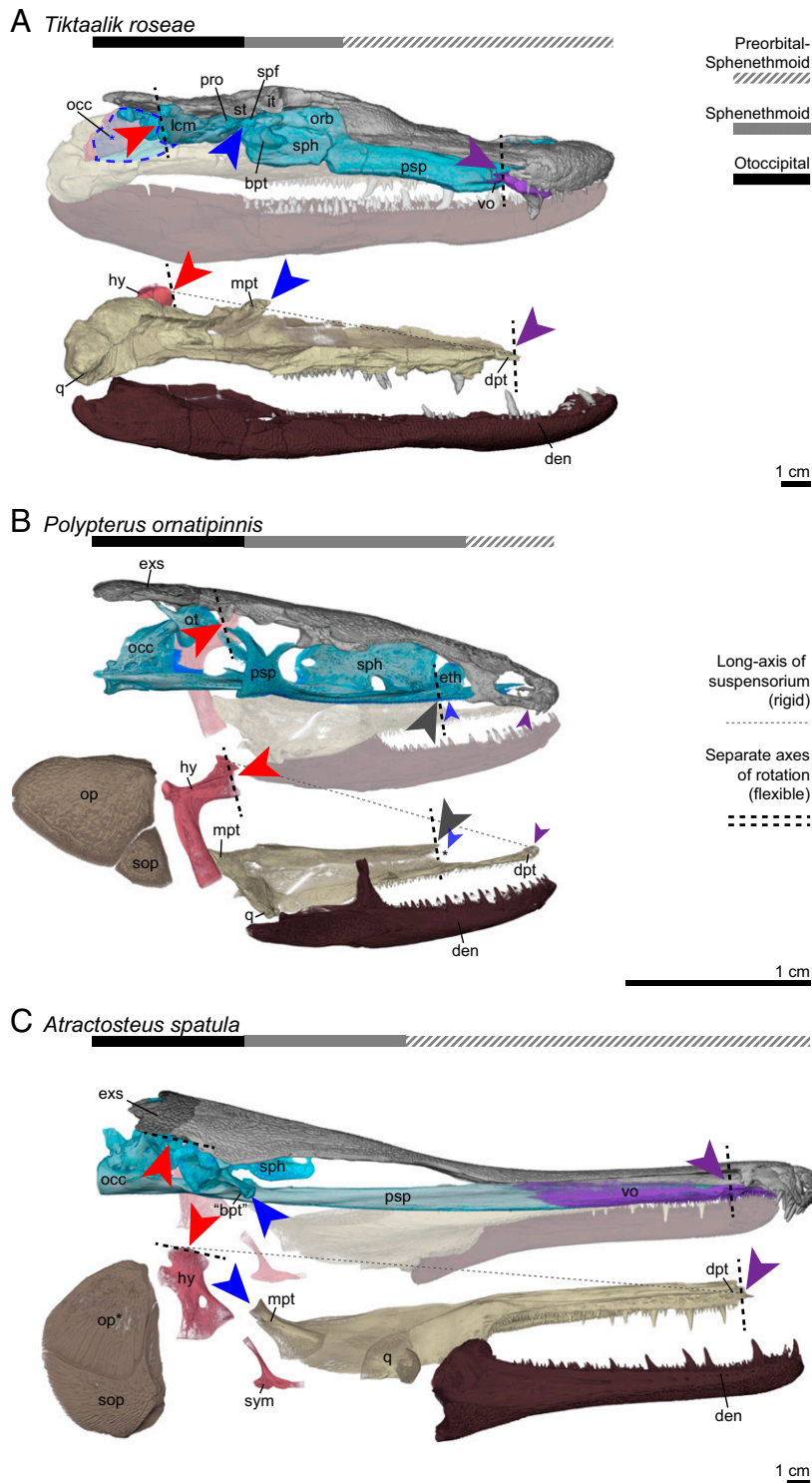https://doi.org/10.1073/pnas.2016421118

Fig. 3. Comparative braincases and suspensoria of *T. roseae* and modern analogs. Right lateral views of the braincases, lower jaws, suspensoria, and opercular bones of (*A*) *T. roseae* (NUFV 108), (*B*) *P. ornatipinnis* (FMNH 117746), and (*C*) *A. spatula* (FMNH 119220D). Skull length has been normalized to the same relative otoccipital length. Published (26) otoccipital–sphenethmoid proportions for NUFV 110 were used for *T. roseae*. Major articulations of the suspensorium are color-coded by element: hyomandibular–otic (red arrows), metapterygoid–basipterygoid (blue arrows), dermopalatine–vomerine (purple arrows), and entopterygoid–parasphenoid (gray arrows, *Polypterus* only). [Asterisk in *B*: Although an autopalatine–ethmoid articulation (small blue arrows) was reported in *Polypterus senegalus* and *Polypterus bichir* (46, 47), no separate autopalatine ossification could be identified in the two specimens of *P. ornatipinnis* that were analyzed.] Dashed lines represent axes of rotation of suspensorial elements (palatoquadrate, hyomandibular) in two conditions: as a single fused functional unit (thin dashed line) or as a flexible system consisting of two functional units (thick dashed lines; *Functional Modularity of the Skull*). bpt, basipterygoid process (nonhomologous between tetrapodomorphs and gar); den, dentary; dpt, dermopalatine; eth, ethmoid; exs, extrascapulars; hy, hyomandibula; it, intertemporal; lcm, lateral commissure; mpt, metapterygoid; occ, occipital region; op, opercle (asterisk in *C*: left side reflected in *A. spatula*); orb, orbit; ot, otic region; pro, prootic buttress; psp, parasphenoid; q, quadrate; sop, subopercle; spf, suprapterygoid fossa; sph, sphenoid region; st, supratemporal; sym, symplectic; vo, vomer.

directly above the vomers. The large entopterygoid has a smooth, weakly ossified, sloping lamina that abuts the sphenethmoid directly ventral to lateral swellings that house the olfactory canals (Fig. 2*A* and *SI Appendix*, Fig. S1*B*). Adjacent to the basipterygoid process, this lamina of the entopterygoid recedes and leaves a prominent notch in the medial side of the palate immediately anterior to the metapterygoid (Fig. 2*A*, asterisk, and Figs. 2*A* and 3*A*, "mpt"). The metapterygoid itself provides the posterior-most articulation of the palate with the braincase in the form of a dorsomedially ascending process that sockets into the suprapterygoid fossa of the braincase (Figs. 2 and 3*A*, "spf," blue arrows, and *SI Appendix*, Fig. S1*C*). The suprapterygoid fossa is largely bounded dorsoposteriorly by the expanded prootic processes and ventroanteriorly by the enlarged basipterygoid processes (Figs. 2*A* and 3*A*). These two processes are enlarged relative to osteolepiforms (26) and, due to dorsoventral compression of the skull, are anatomically closer together than the homologous structures found in *E. foordi* (20). These articulations with the braincase, along with the divisions of the external cheek with the skull roof (see above), indicate the palatoquadrate module is a distinct functional unit capable of motion relative to the midline of the skull.

The hyomandibular module of *T. roseae* is relatively small compared with the other functional units, and consists only of a partially ossified hyomandibula; however, it nevertheless seems to have mobile articulations with the braincase and palate. Proximally, the hyomandibula forms a bifaceted articulation (with distinct dorsal and ventral articular surfaces) with the lateral commissure of the braincase, which is oriented posterolaterally (Figs. 2*A* and 3*A*, "lcm"). These conditions are more similar to tetrapodomorph fishes for which cranial kinesis is assumed to be plesiomorphic (e.g., *Eusthenopteron* and *Panderichthys*) (9, 13) than for limbed tetrapodomorphs (e.g., *Ichthyostega* and *Acanthostega*) (40). The distal end of the hyomandibula is weakly ossified and likely had a primarily cartilaginous articulation with the quadrate (26). As a result, the hyomandibula is only loosely connected to the rest of the suspensorium, and likely allowed some flexibility of movement between it and the "palatoquadrate functional module" (i.e., "intrasuspensorial mobility"; Fig. 3*A*, thick dashed lines).

Last, the "lower jaw module" is important to consider when discussing cranial kinesis because any mediolateral movements of the jaw joint would presumably cause rotation at the mandibular symphysis (Movie S1). The mandibular symphysis of *T. roseae* is smooth and unadorned by rugose ornamentation (*SI Appendix*, Fig. S1*D*), unlike the condition seen in many more derived stem- or crown-group tetrapods (14, 41). Instead, the symphyseal contact was loosely articulated and presumably filled with cartilage and connective tissue, similar to the condition seen in gar and bichir (*SI Appendix*, Fig. S1 *H* and *L*), which are potential modern analogs for understanding tetrapodomorph cranial kinesis (see below).

Modern Analogs. Nonteleost actinopterygian groups are compelling modern analogs for understanding the pattern of moveable joints seen in *T. roseae*. Although sarcopterygian lungfishes and coelacanths are more closely related to modern tetrapods (6), coelacanths have only been studied from preserved specimens (39), and lungfish have evolved an immovable palate ("autostylic") fused to the underside of neurocranium, a highly derived condition relative to finned tetrapodomorphs (6, 19). In contrast, teleostean actinopterygians typically incorporate numerous other moveable elements into their feeding mechanisms, including protrusible premaxillae, depressible maxillae, and/or mechanisms for opercular rotation (1, 4, 36, 42, 43), also highly derived features which tetrapodomorphs lack. However, early diverging actinopterygian groups, such as gars and polypterids, plesiomorphically lack these derived mechanisms (32, 38) and more

closely resemble the morphology of tetrapodomorph fishes (Fig. 3 and *SI Appendix*, Figs. S1, S2, and S3).

Polypterids, including multiple species of *Polypterus* and reedfish (*Erpetoichthys calabaricus*), are frequently used modern analogs for studies into tetrapodomorph feeding mechanisms (5, 44, 45). They possess dorsoventrally compressed cranial anatomy (5, 45), similar to *T. roseae*, and the articulation of the hyomandibula is oriented posteriorly (Fig. 3*B*). While this orientation of the suspensorium was thought to limit lateral expansion in fossil fishes (43), those models assume the suspensorium rotates as a single functional unit (38) (Fig. 3*B*, light dashed line) rather than two. Instead, the hyomandibula has a clear joint with the metapterygoid that suggests some flexibility between elements (Fig. 3*B* and *SI Appendix*, Fig. S2*A*), which may allow separate axes of rotation similar to that reported for gars (34). Lateral expansion of the cheeks is used during suction feeding (5, 38, 45) and spiracular respiration (35). The maxilla and preopercle are interlocking (*SI Appendix*, Fig. S2*B*, "mx " and "pop"), resulting in a cheek that is primarily integrated into the large hyomandibular module of the suspensorium (*SI Appendix*, Fig. S2*A*). The series of cheek bones that overlie the spiracle overlap skull roofing bones, similar to the postorbital bone in *T. roseae* (*SI Appendix*, Figs. S1 *C* and *G* and S2*B*). However, the preorbital, rostral region of *P. ornatipinnis* is markedly divergent from *T. roseae* (Fig. 3*B*). The lacrimal of *P. ornatipinnis* is reduced and seems to form a loosely abutting, "rolling" articulation with the premaxilla (*SI Appendix*, Figs. S1*F* and S2*B*). The slender dermopalatines articulate with a reduced vomer (*SI Appendix*, Fig. S2*A*), but the primary anterior articulation of the palate is at the endopterygoid–parasphenoid articulation medial to the orbits (Fig. 3*B*, gray arrows). The tongue-in-groove morphology of the endopterygoid–parasphenoid articulation (*SI Appendix*, Fig. S1*E*, "ent-psp") suggests only lateral sliding is permitted at this articulation, although further biomechanical studies (such as X-ray Reconstruction of Moving Morphology) will be needed to confirm its mobility compared to the hyomandibula. Despite being reported in other groups of polypterids (46, 47), no separate autopalatine–ethmoid articulation could be identified in *P. ornatipinnis* (Fig. 3*B*, blue arrows). The hyomandibula of *P. ornatipinnis* forms a greater proportion of the suspensorium than in *T. roseae*, and polypterids have no posterior connection of the palate to the braincase (Fig. 3*B*), making them entirely "amphistylic" (i.e., the lower jaws are equally suspended by the palatoquadrate and the hyoid arch) (46).

The alligator gar (*A. spatula*) is a less frequently used model for understanding tetrapodomorph feeding morphology. Unlike polypterids and tetrapodomorphs, only the rostral region of *A. spatula* is dorsoventrally compressed (Fig. 3*C*). The "holostean" hyomandibula is vertically oriented, and the shallow plane of the long axis of the suspensorium (Fig. 3*C*, light dashed line) was thought to limit the range of lateral abduction of the cheek (38); however, the connection between hyosymplectic and palatoquadrate is entirely cartilaginous (32) and forms a flexible, "intrasuspensorial" joint that allows for a much greater range of motion during lateral abduction of the palate (34). The preopercle, quadratojugal, and circumorbitals are integrated with the hyosymplectic into a hyomandibular module (*SI Appendix*, Fig. S3*B*), which is suspended from the dermatocranium in a simple hinge (*SI Appendix*, Figs. S1*K* and S3, "coh"). In contrast, the lacrimomaxillae are sutured to the bones of the palate (*SI Appendix*, Fig. S1*J*) and are thus part of the palatoquadrate module, which can be seen flexing relative to the circumorbitals during feeding (34). The palate and rostrum share many convergent similarities with *T. roseae*. The preorbital rostral region of the sphenethmoid is elongated to a similar degree as *T. roseae*, placing the anterior connection of the palate to the braincase far anteriorly (Fig. 3*C* and *SI Appendix*, Fig. S3, purple arrows). This

Lemberg et al.
The feeding system of *Tiktaalik roseae*: an intermediate between suction feeding and biting

PNAS | 5 of 10
https://doi.org/10.1073/pnas.2016421118

connection consists of a small prong of the dermopalatine that fits into a posteriorly facing socket formed by the premaxilla and vomers (*SI Appendix*, Fig. S1*I*). The premaxilla and frontals form an elongate, nonsutural scarf joint with the palate and lacrimomaxillae (*SI Appendix*, Figs. S1*J* and S3*B*, magenta line) that spreads apart during lateral sliding of the palate (34). The posterior connection of the palate is a sliding joint with the metapterygoid and a convergently evolved basipterygoid process (Fig. 3*C* and *SI Appendix*, Fig. S3*A*, "bpt," blue arrows) that is unique to gars among actinopterygians (32, 33, 46). Similar to *T. roseae*, the enlarged palate of *A. spatula* has no bony contact with the hyomandibula, making it a mobile but essentially autostylic jaw suspension (Fig. 3*C*).

Discussion

Numerous anatomical features suggest that the skull of *T. roseae* was modified for prey capture through biting. The skull is dorsoventrally compressed, the palate is horizontally oriented (25, 26), and lateral cheek bones have overlapping sutures, features that have been interpreted to be convergent with lateral snapping crocodilians (10, 21, 22, 31, 48). The prevalence of interdigitating and complex sutures along the midline of the dermatocranium (Fig. 1) is similar to the pattern seen in *A. gunnari* and has been interpreted as a modification for resisting biting forces (5, 21). The neurocranium is consolidated relative to fish-like ancestors as well, with advancement of the prootics (Fig. 2*A*, "pro") anterior to the intracranial joint (Fig. 2*B*, "icj"). The snout and jaws are elongate (Fig. 3*A*), with no suggestion of fleshy lobes, such as found in polypterids (44), to occlude the

corners of the mouth and facilitate forceful, directed suction (1, 48–50). Instead, the tooth row extends posteriorly lateral to the adductor chamber (Fig. 2*A*, "dltr") in a manner highly suggestive of lateral snapping similar to gars (34, 38, 51). These findings, along with loss of the bony operculum, reduction of the hyomandibula, and enlargement of the basipterygoid process (Fig. 3*A*, "bpt"), have led to the hypothesis that suction played a reduced role in prey capture in *T. roseae* and later tetrapodomorphs (26, 40).

However, µCT of *T. roseae* also reveals surprising indicators of kinetic capabilities throughout the cranium, particularly in the joints between the cheek, palate, and braincase. Despite significant restructuring and consolidation of the skull, the cheek retains a nonsutural connection to the braincase that is anteriorly similar to *A. spatula* (*SI Appendix*, Fig. S1 *B* and *J*) and postorbitally similar to *P. ornatipinnis* (*SI Appendix*, Fig. S1 *C* and *G*). The enlarged palate of *T. roseae* has mobile attachments to the braincase that are convergently evolved with *A. spatula* despite reduction of the hyomandibular component of the suspensorium (Fig. 3 *A* and *C*). With a relatively loose connection between the hyomandibular and palatoquadrate functional components of the suspensorium, it is possible these elements had separate axes of rotation (Figs. 3*A* and 4*A*), as proposed for other nondipnoan sarcopterygian fishes (9, 39). Whereas the expanded basipterygoid process has been interpreted to limit movement of the metapterygoid (i.e., epipterygoid) dorsoventrally relative to the braincase (26), it might have nevertheless provided an expanded surface for the metapterygoid to slide laterally (in the same direction permitted by the scarf joints) without disarticulation, as
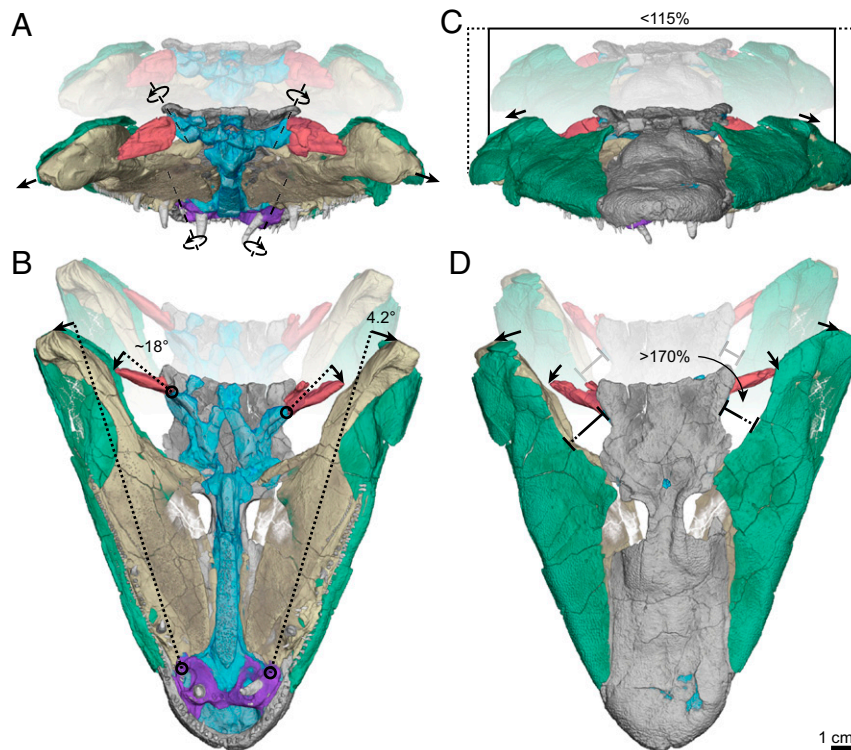

Fig. 4. Proposed expansion of the feeding and respiratory systems of *T. roseae* due to cranial kinesis. Faded background shows the resting state, whereas the in-focus foreground shows reconstructed estimates of the fully expanded state. (*A*) Posterior view showing the independent axes of rotation for the hyomandibulae (red) and palatoquadrate (yellow). Joint morphology suggests these elements rotate/slide laterally, as indicated here by dorsolaterally oriented axes. (*B*) Ventral view showing that small rotation of the dermopalatine–vomer joint (4.2°) results in large posterior rotation of the palatoquadrate and hyomandibula (18°). (*C*) Anterior view showing that lateral sliding of the cheek (green) along with the palate results in modest expansion of the opercular cavities (<15% increase of the resting width of the skull). (*D*) Dorsal view showing that lateral rotation of the palate and hyomandibula results in pronounced expansion of the spiracles (>70% increase of the width of the spiracle distance in dorsal view).

in gar (34). Together, these features could serve to expand the buccal cavities during feeding.

Recognizing analogous features in the feeding systems of *T. roseae* and *A. spatula* enables the application of alligator gar cranial kinematics (34) to tetrapodomorph morphology, with implications for the evolution of tetrapodomorph feeding and respiratory strategies. Joint morphology in *T. roseae* indicates that, while restricted in dorsoventral movements, lateral abduction of the cheek and palate would have been possible (Fig. 4 and Movie S1). Lateral abduction of the cheek and palate is important not only for expanding the pharynx in osteichthyans, it also drives lateral abduction of the gill bars and operculum (1, 37). The loss of the bony operculum in *T. roseae* and limbed tetrapodomorphs is thought to represent a shift away from aquatic respiration (26) due to loss of the opercular pump (37); however, respiratory gills persist well into the tetrapod stem (52, 53), suggesting that, even after loss of the operculum, ventilation occurred through buccal pumping (6, 37). In *T. roseae*, modest expansion of the opercular cavity occurs through lateral sliding of the cheek and palate (an increase of ~15% of the resting width of the skull; Fig. 4C) and might have been sufficient to expand the opercular flap and overcome passive resistance of the gills to the posterior flow of water (37). Although the extent of opercular expansion in this system is limited by the length of the hyomandibulae and the horizontal orientation of the palate (Fig. 4C), these movements nevertheless produce substantial expansion of the spiracular canal (>70%; Fig. 4D). Spiracular respiration has been described as being an intermediate stage between opercular pumping and buccal respiration (27, 35, 40). The retention of cranial kinesis in *T. roseae* would have enhanced the ability to use the spiracles in feeding and respiration, similar to polypterids (35), while simultaneously supporting the use of a combined snapping-and-suction feeding strategy in water, similar to gars (34).

The retention of cranial kinesis in *T. roseae* supports the hypothesis that more derived examples of cranial kinesis in the tetrapod stem and crown group were inherited from osteolepiform tetrapodomorph ancestors (13, 14, 18). The system of cranial kinesis proposed here for *T. roseae* is largely similar to those proposed for osteolepiforms (9), albeit with modifications for closure of the intracranial joint, dorsoventral compression, rostral elongation, and autostyly. Although there are multiple independent losses of cranial kinesis in various groups [e.g., ichthyostegids (54) and whatcheeriids (41)], there are also multiple groups that appear to retain mobility [e.g., baphetids (15), embolomeres (17), and colosteids (14)]. Cranial kinesis in *T. roseae* reveals a transitional stage in which an amphistylic, fish-like system (9) has acquired features that reveal a shift toward a more autostylic, tetrapod-like system of kinesis (13) (Fig. 5). While it is still uncertain if early limbed tetrapodomorphs retained cranial kinesis, with vomers incorporated into the palate (19) and further reduced hyomandibulae (55, 56) (Fig. 5), future studies may benefit from reexamination of the joints and articular surfaces determined here as being integral to cranial kinesis in *T. roseae*.

Whereas most studies of the evolution of function in the feeding systems of early tetrapods have focused on whether taxa were capable of either suction or biting, functionally trading off one for the other (2, 5, 7, 8), we argue that understanding the shift in feeding strategies at the water-to-land transition requires a more nuanced perspective. There is increasing evidence from modern taxa that these feeding strategies may actually be synergistic and in fact overlap significantly in functional morphospace (36, 57). Therefore, perhaps the evolution of the tetrapod feeding system should be viewed as a gradual transition through a series of local peaks in an adaptive landscape (58), rather than as a strict dichotomy. As demonstrated by gar (34), adaptations for biting can be elaborated while effective suction generation is maintained (36), and many of the analogous features seen in *T. roseae*, such as the evolution of an enlarged basipterygoid process, rostral elongation, fusion of the neurocranium through advancement of the prootics, and transition to an autostylic suspensory system (possibly freeing the role of the hyomandibula for its eventual incorporation into the auditory system), are some of the most quintessential features of early tetrapod cranial anatomy (6) (Fig. 5). A gar-like stage in aquatic animals such as *T. roseae* may have been an important transitional step in the evolution of the biting-based feeding system that facilitated prey capture on land by the earliest terrestrial vertebrates.
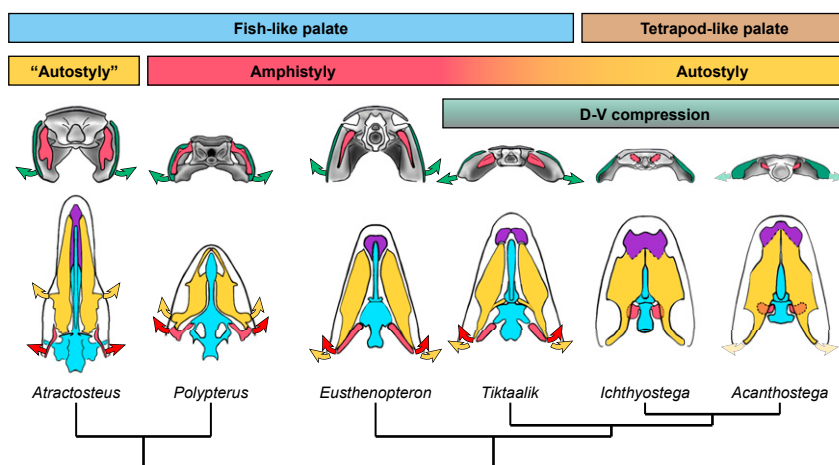
Fig. 5. Intermediate conditions in the feeding system of *T. roseae*. Shown are posterior (top row) and ventral (bottom row) views of *T. roseae* and comparative taxa. *T. roseae* maintains a palatal configuration similar to other fish, with the palate (yellow) maintaining a mobile joint with the vomers (purple). In contrast, later tetrapodomorphs (*Ichthyostega*, *Acanthostega*) have palates that meet at the midline and incorporate the vomers into the functional palate. Modern analogs show how some elpistostegalian traits—in *Atractosteus*, rostral elongation with a large, horizontal palate supported posteriorly by an enlarged basipterygoid process (a precursor to the autostylic suspensoria of later tetrapodomorphs); or, in *Polypterus*, dorsoventrally flattened skull with posteriorly directed hyomandibulae—do not preclude cranial kinesis (arrows). Although hyomandibular mobility (red arrows) is no longer a contributor to cranial kinesis in autostylic tetrapods, it is possible the cheek (green arrows) and palate (yellow arrows) may still retain some mobility across the fish–tetrapod transition in some taxa (faded arrows).

Lemberg et al.
The feeding system of *Tiktaalik roseae*: an intermediate between suction feeding and biting

PNAS | 7 of 10
https://doi.org/10.1073/pnas.2016421118

Materials and Methods

Using μCT, we reconstructed the internal morphology, joints, and dermal sutures of the external cheek, palate, skull table, and braincase of *T. roseae*. Comparing taphonomic patterns between multiple specimens allowed for limited retrodeformation of the relatively intact holotype skull (NUFV 108). This 3D digital reconstruction was then manipulated into the various stages of the feeding sequences of a modern fish analog, *A. spatula* (alligator gar), using published data of gar kinematics (34).

μCT. Cranial μCT data were collected for six specimens of *T. roseae* and two specimens of *P. ornatipinnis* (*SI Appendix*, Table S1). The scans were collected using the UChicago PaleoCT (GE Phoenix v|tome|x 240-kv/180-kv scanner; luo-lab.uchicago.edu/paleoCT.html). Additionally, cranial μCT data were also collected for one adult alligator gar (*A. spatula*) scanned at the GE Training Facility in Lewistown, PA, using a GE Phoenix v|tome|x 240-kv/180-kv scanner (*SI Appendix*, Table S1). Scanning parameters were optimized for internal details, which, in these specimens, favored lower (<100 keV) voltage, higher current, and less filtration. However, these same parameters also reduced surface contrast and increased the prevalence of some scanning artifacts (including beam hardening). In cases where sutures were not visible, the specimen was rescanned using adjusted scanning parameters.

Digital Segmentation. μCT scans were analyzed in Amira 2020.2 (FEI). Segmentations emphasized bones, sutures, and joints of interest for elucidating the feeding mechanism. Visualization in Amira 2020.2 incorporated volume renderings of the individually segmented cranial elements, with color coding based on the region of the skull the element belonged to: cheeks (green), palate (yellow), braincase (cyan), dermatocranium (gray), vomers (purple), hyomandibulae (red), and preopercle (pink).

Assessing Sutural Morphology. Sutural contact between bones was examined referencing μCT data of all available *T. roseae* specimens (*SI Appendix*, Table S1). Specific sutures were chosen to directly compare with those reported in *E. foordi* (5, 20) and *A. gunnari* (5, 21, 23); however, these were supplemented with other sutures and joints deemed suitable for analysis (Fig. 1). Terminology of sutures used here are made in reference to other studies that include sutural analyses (5, 21, 23), but departs with these studies when referring to the anatomical division between the cheek and the skull roof (Fig. 1). These articulations are deemed nonsutural due to their location along a primitive anatomical divide among sarcopterygians (20), as well as due to the presence of matrix in-fill in μCT cross-section (Fig. 1), likely the result of a loose articulation in life similar to modern alligator gar (34) (*SI Appendix*, Fig. S1J, "fr-ect"). This contrasts with other sutural scarf joints found throughout the cranium of *T. roseae* (Fig. 1, red lines) and *A. spatula* (*SI Appendix*, Fig. S1J) where bone–bone contact is overlapping but also tightly articulating.

Limited Retrodeformation. Due to preservational differences between the multiple *T. roseae* specimens, it can be assumed that each specimen experienced some postmortem deformation. The skull of NUFV 110 is taller than that of NUFV 108, the cheek overlaps the dermatocranium to a greater degree, and the articulated jaws have been shifted to one side. For this reason, we assumed that the skull of NUFV 110 has been laterally compressed (*SI Appendix*, Fig. S4) relative to NUFV 108. In comparison, the palates, cheeks, hyomandibulae, and lower jaws of NUFV 108 appear to have been dorsally compressed (*SI Appendix*, Fig. S5), and, in order to create a more lifelike condition, elements of the skull of NUFV 108 were repositioned to conform more to conditions found in the other specimens. Lifelike positions of cranial elements of *T. roseae* were the result of rotation and translations only, with no use of scaling or plastic deformation to reposition any element.

Specifically, the cheeks and palates of NUFV 108 were rotated slightly ventromedially from their splayed in situ positions (*SI Appendix*, Fig. S6). The left and right cheeks were elevated dorsally (relative to the *x* and *z* axes; *SI Appendix*, Fig. S7 *A–D*) and brought into contact with the dermatocranium in order to close the gap left by the nonsutural joint between the cheek and braincase (Fig. 1 *F* and *H*). The left and right palates were rotated dorsally in the *z* axis and each rotated slightly from left to right to make them symmetrical to the midline (*SI Appendix*, Fig. S7 *E* and *F*). This brought the lateral dorsal surfaces of the palates horizontal as well as brought the palatal toothrows of the ectopterygoid and dermopalatine into alignment with the maxillary toothrows [as depicted in other taxa (20, 21, 23, 40, 54, 59)]. The hyomandibulae were rotated inward along their long axes in order to bring their articular facets more in line with the articular surfaces of the lateral

commissures (*SI Appendix*, Fig. S7D). Transformation matrices for each cranial element were exported from Amira 2020.2 and are provided in *SI Appendix*, Table S2. Additionally, a video is provided showing the results of retrodeformation in each of the cardinal views (Movie S2).

The result was a more lifelike anatomical model of *T. roseae*, with a marginally taller skull and slightly vaulted palate (*SI Appendix*, Fig. S7), which represents our current best understanding of the original shape of the skull. Nevertheless, despite the attention to anatomical detail and usage of up-to-date reconstruction methods, in the absence of a perfectly 3D-preserved specimen, this model still contains some uncertainties. In particular, it is likely the posterior neurocranium and dermatocranium experienced dorsoventral compression as well, but since the skull roof and sphenethmoid regions of the braincase (where the palates and cheek attach) are well ossified, no attempts were made to heighten the skull for this study.

Three-Dimensional Animation. Repositioned cranial elements in the retrodeformed model were used to animate cranial kinesis in *T. roseae*. Each functional module (neurocranial, palatoquadrate, hyomandibular) of the *T. roseae* skull was given its own axis of rotation and range of motion based on analogous modules and kinematics reported for *A. spatula* (34). For the palatoquadrate module, the cheeks were allowed to rotate at the maxilla–premaxilla junction and slide ventrolaterally in the direction indicated by the slope of the rostral scarf joint and the prootic shelf (Figs. 1 *D*, *F*, and *H* and F2*B*, "rsj" and "proshf," respectively). The palates were rotated to match these movements of the cheek at the vomer–dermopalatine joint (Fig. 4B). A maximum of 4.6° of rotation was possible without disarticulating the joints of the cheek and skull roof (*SI Appendix*, Fig. S8F), which was seen as the limit to which the cheeks could expand (Fig. 4C). Then, the hyomandibulae (hyomandibular module) were rotated around their articular axes with the lateral commissures of the braincase in order to maintain their corresponding orientation with the palatoquadrates (Fig. 4D). Finally, rotation matrices that define movement for these elements around fixed anatomical landmarks were exported, corresponding to the resting and expanded states (*SI Appendix*, Table S3), and the animation software in Amira 2020.2 was used to smoothly interpolate between these matrices in order to create the animation (Movie S1).

Use of Modern Analogs. One of the primary concerns when applying insights gained from modern analogs to the fossil record is how applicable those data are in the absence of soft tissue. While soft tissues restrict the range of motion of kinematic systems in living organisms, the extent of soft tissues can only be inferred in fossil taxa. Furthermore, computer modeling that lacks these necessary data as input can become unconstrained and typically overestimate the range of motion of kinematic systems.

In the study on alligator gar feeding mechanics, this problem was addressed by using a conservative two-pronged approach (34). First, in vivo feeding kinematics provided the kinematic range and average values for the extent of cranial expansion due to cranial kinesis. Second, a 3D linkage computer model of feeding kinematics was built using a specimen fixed in an expanded state and scanned using contrast-enhanced μCT, thus producing kinematics that were verified to not dislocate any soft tissue (34).

As a result, the kinematic values used to reconstruct palatal movements in *T. roseae* represent a conservative and in vivo-validated measurement of typical suspensorial abduction in a long-snouted modern analog for which soft tissue was taken into account (alligator gar). Nevertheless, this range of motion appears to strain the limits of articulated cranial expansion in *T. roseae* (*Three-Dimensional Animation* and Movie S1), and therefore it likely represents an extreme range of motion for this fossil taxon.

Measuring Expansive Variables. Due to the lack of preserved soft tissue, such as an opercular flap or spiracular valve, the exact volumes of the opercular cavity and spiracular canal could not be measured. Instead, these analyses used simple linear measurements that can be directly compared with other taxa for which there are available data on spiracular and opercular expansion (34, 35). For expansion of the opercular region, we measured the width of the skull before and after lateral expansion (Fig. 4C):

$$\text{Opercular expansion }(\%) = (\text{expanded cranial width}/\text{resting cranial width}) \times 100$$

In gar, these measurements (using the width of the skull at the preopercles) averaged 44.9% ± 7.6 expansion due to cranial kinesis, which is a value greater than that estimated for *T. roseae* (~15%; *Discussion*). For spiracular expansion, we measured the width of the spiracle at its widest

point in dorsal view perpendicular to the long axis of the spiracle before and after cranial expansion (Fig. 4*D*):

$$\text{Spiracular expansion (\%)} = (\text{expanded spiracular width/resting spiracular width}) \times 100$$

Unfortunately, in *Polypterus*, the spiracular flap covers the spiracular cavity, and there are as of yet no in vivo studies that measure the change in shape of the spiracular canal due to cranial kinesis. Future studies capable of measuring positional differences between the palate and hyomandibula (such as X-ray Reconstruction of Moving Morphology or sonomicrometry) will be needed to directly measure this kinematic variable in a living polypterid.

Data Availability. Micro-CT data for *T. roseae* (NUFV 108, 109, 110, 111, 119, 149), *P. ornatipinnis* [Field Museum of Natural History (FMNH) 117746, 121744], and *A. spatula* (FMNH 119220D) are available on MorphoSource (P1213) (60) (*SI Appendix*, Table S1).

1. P. C. Wainwright, M. D. McGee, S. J. Longo, L. P. Hernandez, Origins, innovations, and diversification of suction feeding in vertebrates. *Integr. Comp. Biol.* **55**, 134–145 (2015).
2. S. Van Wassenbergh, "Transitions from water to land: Terrestrial feeding in fishes" in *Feeding in Vertebrates: Evolution, Morphology, Behavior, Biomechanics*, V. Bels, I. Q. Whishaw, Eds. (Springer International Publishing, Cham, 2019), pp. 139–158.
3. E. Heiss, P. Aerts, S. Van Wassenbergh, Aquatic-terrestrial transitions of feeding systems in vertebrates: A mechanical perspective. *J. Exp. Biol.* **221**, jeb154427 (2018).
4. S. Van Wassenbergh et al., Evolution: A catfish that can strike its prey on land. *Nature* **440**, 881 (2006).
5. M. J. Markey, C. R. Marshall, Terrestrial-style feeding in a very early aquatic tetrapod is supported by evidence from experimental analysis of suture morphology. *Proc. Natl. Acad. Sci. U.S.A.* **104**, 7134–7138 (2007).
6. J. A. Clack, *Gaining Ground: The Origin and Evolution of Tetrapods* (Indiana University Press, 2012).
7. J. M. Neenan, M. Ruta, J. A. Clack, E. J. Rayfield, Feeding biomechanics in *Acanthostega* and across the fish–tetrapod transition. *Proc. Biol. Sci.* **281**, 20132689 (2014).
8. P. S. L. Anderson, M. Friedman, M. Ruta, Late to the table: Diversification of tetrapod mandibular biomechanics lagged behind the evolution of terrestriality. *Integr. Comp. Biol.* **53**, 197–208 (2013).
9. K. S. Thomson, Mechanisms of intracranial kinetics in fossil rhipidistian fishes (Crossopterygii) and their relatives. *Zool. J. Linn. Soc.* **46**, 223–253 (1967).
10. A. B. Busbey III, "The structural consequences of skull flattening in crocodilians" in *Functional Morphology in Vertebrate Paleontology*, J. J. Thomason, Ed. (Cambridge University Press, Cambridge, UK, 1995), pp. 173–192.
11. J. Fortuny et al., 3d bite modeling and feeding mechanics of the largest living amphibian, the Chinese giant salamander *Andrias davidianus* (Amphibia:Urodela). *PLoS One* **10**, e0121885 (2015).
12. J. Fortuny, J. Marcé-Nogué, S. DE Esteban-Trivigno, L. Gil, Á. Galobart, Temnospondyli bite club: Ecomorphological patterns of the most diverse group of early tetrapods. *J. Evol. Biol.* **24**, 2040–2054 (2011).
13. N. N. Iordansky, Evolution of cranial kinesis in lower tetrapods. *Neth. J. Zool.* **40**, 32–54 (1990).
14. J. R. Bolt, R. E. Lombard, The mandible of the primitive tetrapod *Greererpeton*, and the early evolution of the tetrapod lower jaw. *J. Paleontol.* **75**, 1016–1042 (2001).
15. E. H. Beaumont, Cranial morphology of the Loxommatidae (Amphibia: Labyrinthodontia). *Philos. Trans. R. Soc. Lond. B Biol. Sci.* **280**, 29–101 (1977).
16. A. L. Panchen, On the amphibian *Crassigyrinus scoticus* Watson from the Carboniferous. *Philos. Trans. R. Soc. Lond. B Biol. Sci.* **309**, 505–568 (1985).
17. A. L. Panchen, The cranial anatomy of two Coal Measure anthracosaurs. *Philos. Trans. R. Soc. Lond. B Biol. Sci.* **247**, 593–636 (1964).
18. R. E. Lombard, J. R. Bolt, Evolution of the tetrapod ear: An analysis and reinterpretation. *Biol. J. Linn. Soc. Lond.* **11**, 19–76 (1979).
19. D. E. Rosen, P. L. Forey, B. G. Gardiner, C. Patterson, Lungfishes, tetrapods, paleontology, and plesiomorphy. *Bull. AMNH* **167**, 4 (1981).
20. E. Jarvik, *Basic Structure and Evolution of Vertebrates* (Academic Press, New York, NY, 1980).
21. J. A. Clack, The dermal skull roof of *Acanthostega gunnari*, an early tetrapod from the Late Devonian. *Earth Environ. Sci. Trans. R. Soc. Edinb.* **93**, 17–33 (2002).
22. P. E. Ahlberg, Follow the footprints and mind the gaps: A new look at the origin of tetrapods. *Earth Environ. Sci. Trans. R. Soc. Edinb.* **109**, 1–23 (2018).
23. L. B. Porro, E. J. Rayfield, J. A. Clack, Descriptive anatomy and three-dimensional reconstruction of the skull of the early tetrapod *Acanthostega gunnari* Jarvik, 1952. *PLoS One* **10**, e0118882 (2015).
24. L. B. Porro, E. J. Rayfield, J. A. Clack, Computed tomography, anatomical description and three-dimensional reconstruction of the lower jaw of *Eusthenopteron foordi* Whiteaves, 1881 from the Upper Devonian of Canada. *Paleontology* **58**, 1031–1047 (2015).
25. E. B. Daeschler, N. H. Shubin, F. A. Jenkins Jr, A Devonian tetrapod-like fish and the evolution of the tetrapod body plan. *Nature* **440**, 757–763 (2006).
26. J. P. Downs, E. B. Daeschler, F. A. Jenkins, Jr, N. H. Shubin, The cranial endoskeleton of *Tiktaalik roseae*. *Nature* **455**, 925–929 (2008).
27. P. A. Beznosov, J. A. Clack, E. Lukševičs, M. Ruta, P. E. Ahlberg, Morphology of the earliest reconstructable tetrapod *Parmastega aelidae*. *Nature* **574**, 527–531 (2019).
28. J. D. Pardo, M. Szostakiwskyj, P. E. Ahlberg, J. S. Anderson, Hidden morphological diversity among early tetrapods. *Nature* **546**, 642–645 (2017).
29. P. E. Ahlberg, J. A. Clack, Lower jaws, lower tetrapods–a review based on the Devonian genus *Acanthostega*. *Earth Environ. Sci. Trans. R. Soc. Edinb.* **89**, 11–46 (1998).
30. P. E. Ahlberg, J. A. Clack, E. Luksevics, Rapid braincase evolution between *Panderichthys* and the earliest tetrapods. *Nature* **381**, 61–64 (1996).
31. B. Hohn-Schulte, H. Preuschoft, U. Witzel, C. Distler-Hoffmann, Biomechanics and functional preconditions for terrestrial lifestyle in basal tetrapods, with special consideration of *Tiktaalik roseae*. *Hist. Biol.* **25**, 167–181 (2013).
32. L. Grande, An empirical synthetic pattern study of gars (Lepisosteiformes) and closely related species, based mostly on Skeletal Anatomy: The resurrection of Holostei. *Copeia* **2011**, 612–613 (2010).
33. M. Jollie, Development of cranial and pectoral girdle bones of *Lepisosteus* with a note on scales. *Copeia* **1984**, 476–502 (1984).
34. J. B. Lemberg, N. H. Shubin, M. W. Westneat, Feeding kinematics and morphology of the alligator gar (*Atractosteus spatula*, Lacépède, 1803). *J. Morphol.* **280**, 1548–1570 (2019).
35. J. B. Graham et al., Spiracular air breathing in polypterid fishes and its implications for aerial respiration in stem tetrapods. *Nat. Commun.* **5**, 3022 (2014).
36. A. C. Gibb, L. Ferry-Graham, Cranial movements during suction feeding in teleost fishes: Are they modified to enhance suction production? *Zoology (Jena)* **108**, 141–153 (2005).
37. E. L. Brainerd, L. A. Ferry-Graham, "Mechanics of respiratory pumps" in *Fish Physiology*, E. S. Robert, V. L. George (Academic Press, 2005), vol. 23, pp 1–28.
38. G. V. Lauder Jr., Evolution of the feeding mechanism in primitive actionopterygian fishes: A functional anatomical analysis of *Polypterus*, *Lepisosteus*, and *Amia*. *J. Morphol.* **163**, 283–317 (1980).
39. H. Dutel, A. Herrel, G. Clément, M. Herbin, Redescription of the hyoid apparatus and associated musculature in the extant coelacanth *Latimeria chalumnae*: Functional implications for feeding. *Anat. Rec. (Hoboken)* **298**, 579–601 (2015).
40. M. D. Brazeau, P. E. Ahlberg, Tetrapod-like middle ear architecture in a Devonian fish. *Nature* **439**, 318–321 (2006).
41. R. E. Lombard, J. R. Bolt, M. T. Carrano, "The mandible of *Whatcheeria deltae*, an early tetrapod from the Late Mississippian of Iowa" in *Amniote Paleobiology. Perspectives on the Evolution of Mammals, Birds, and Reptiles*, M. T. Carrano, T. J. Gaudin, R. W. Blob, J. R. Wi, Eds. (University of Chicago Press, Chicago, IL, 2006), pp. 21–52.
42. K. B. Michel, D. Adriaens, P. Aerts, M. Dierick, S. V. Wassenbergh, Functional anatomy and kinematics of the oral jaw system during terrestrial feeding in *Periophthalmus barbarus*. *J. Morphol.* **275**, 1145–1160 (2014).
43. B. Schaeffer, D. E. Rosen, Major adaptive levels in the evolution of the actinopterygian feeding mechanism. *Am. Zool.* **1**, 187–204 (1961).
44. S. Van Wassenbergh, C. Bonte, K. B. Michel, Terrestrial capture of prey by the reedfish, a model species for stem tetrapods. *Ecol. Evol.* **7**, 3856–3860 (2017).
45. M. J. Markey, R. P. Main, C. R. Marshall, In vivo cranial suture function and suture morphology in the extant fish *Polypterus*: Implications for inferring skull function in living and fossil fish. *J. Exp. Biol.* **209**, 2085–2102 (2006).
46. G. Arratia, H.-P. Schultze, Palatoquadrate and its ossifications: Development and homology within osteichthyans. *J. Morphol.* **208**, 1–81 (1991).
47. M. Jollie, Development of the head and pectoral skeleton of *Polypterus* with a note on scales (Pisces: Actinopterygii). *J. Zool.* **204**, 469–507 (1984).
48. M. A. Taylor, How tetrapods feed in water: A functional analysis by paradigm. *Zool. J. Linn. Soc.* **91**, 171–195 (1987).
49. R. J. Damiani, Cranial anatomy of the giant Middle Triassic temnospondyl *Cherninia megarhina* and a review of feeding in mastodonsaurids. *Palaeont. Afr.* **37**, 41–52 (2001).

EVOLUTION

Lemberg et al.
The feeding system of *Tiktaalik roseae*: an intermediate between suction feeding and biting

PNAS | 9 of 10
https://doi.org/10.1073/pnas.2016421118

50. F. Witzmann, R. R. Schoch, Reconstruction of cranial and hyobranchial muscles in the Triassic temnospondyl *Gerrothorax* provides evidence for akinetic suction feeding. *J. Morphol.* **274**, 525–542 (2013).

51. H. T. Porter, P. J. Motta, A comparison of strike and prey capture kinematics of three species of piscivorous fishes: Florida gar (*Lepisosteus platyrhincus*), redfin needlefish (*Strongylura notata*), and great barracuda (*Sphyraena barracuda*). *Mar. Biol.* **145**, 989–1000 (2004).

52. M. I. Coates, J. A. Clack, Fish-like gills and breathing in the earliest known tetrapod. *Nature* **352**, 234–236 (1991).

53. R. R. Schoch, F. Witzmann, Bystrow's Paradox – gills, fossils, and the fish-to-tetrapod transition. *Acta Zool.* **92**, 251–265 (2010).

54. E. Jarvik, The Devonian tetrapod *Ichthyostega. Lethaia* **29**, 76 (1996).

55. J. A. Clack, Earliest known tetrapod braincase and the evolution of the stapes and Fenestra Ovalis. *Nature* **369**, 392–394 (1994).

56. J. A. Clack *et al.*, A uniquely specialized ear in a very early tetrapod. *Nature* **425**, 65–69 (2003).

57. S. J. Longo, M. D. McGee, C. E. Oufiero, T. B. Waltzek, P. C. Wainwright, Body ram, not suction, is the primary axis of suction-feeding diversity in spiny-rayed fishes. *J. Exp. Biol.* **219**, 119–128 (2016).

58. B. V. Dickson, S. E. Pierce, Functional performance of turtle humerus shape across an ecological adaptive landscape. *Evolution* **73**, 1265–1277 (2019).

59. J. R. Bolt, R. E. Lombard, Palate and braincase of *Whatcheeria deltae* Lombard & Bolt, 1995. *Earth Environ. Sci. Trans. R. Soc. Edinb.* **109**, 177–200 (2019).

60. J. B. Lemberg, E. B. Daeschler, N. H. Shubin, Project: The feeding system of Tiktaalik roseae: an intermediate between suction feeding and biting. MorphoSource, P1213. https://www.morphosource.org/Detail/ProjectDetail/Show/project_id/1213. Accessed 16 December 2020.